Limnol. Oceanogr., 59(5), 2014, 1704–1714

doi:10.4319/lo.2014.59.5.1704

Dispersal pathways of American eel larvae from the Sargasso Sea

Irina I. Rypina,[1,*] Joel K. Llopiz,[2] Lawrence J. Pratt,[1] and M. Susan Lozier [3]

[1] Physical Oceanography Department, Woods Hole Oceanographic Institution, Woods Hole, Massachusetts
[2] Biology Department, Woods Hole Oceanographic Institution, Woods Hole, Massachusetts
[3] Earth and Ocean Sciences, Nicholas School of the Environment, Duke University, Durham, North Carolina

Abstract

At the end of their life cycle, American eel (*Anguilla rostrata*) migrate to the Sargasso Sea from freshwater habitats along the east coast of North America in order to spawn planktonic eggs. The eggs develop into larvae that then have to reach estuarine and freshwater nursery habitats along the North American coast within approximately their first year of life. A coupled biological–physical model was used to study how potential behavioral adaptations influence the ability of American eel larvae to reach near-coastal waters. Specifically, several larval swimming behaviors were investigated, including passive drift, random walk swimming, and directional navigation with and without a preferred swimming direction. Directional swimming with a randomly chosen direction improved the success rates of larvae reaching the continental shelf by more than two orders of magnitude compared to passive drift, and swimming primarily to the northwest further tripled these success rates. Success rates also substantially increased for larvae with swimming abilities even slightly above an estimated average. Notably, directional swimming resulted in a reasonable distribution of larvae along the North American shelf break, whereas other swimming scenarios left distinct gaps where no simulated larvae reached the shelf, including near the Gulf of Maine where juvenile eels are abundant. Additionally, directional swimming yielded transit times of ~ 1 yr, in agreement with observations. Finally, the model supported the southwestern Sargasso Sea as the probable spawning area for American eel.

Marine larval dispersal, which is a result of the interaction between ecological and physical processes (Epifanio and Garvine 2001; Levin 2006; Cowen and Sponaugle 2009), has been investigated for a wide variety of systems and species (Hare et al. 2002; Melià et al. 2013; Pacariz et al. 2014). An overwhelming majority of fishes and invertebrates in oceanic and coastal waters exhibit a reproductive strategy characterized by a pelagic larval stage, with each adult spawning hundreds to millions of eggs that then hatch into small planktonic larvae. This strategy makes for a bipartite life history, whereby adult and juvenile sizes, behavior, and habitat are entirely distinct from those of the millimeter-scale eggs and larvae, which are, to varying degrees, at the mercy of the currents in which they are entrained. Larvae (especially those in the earliest days of development) are thus highly susceptible to being swept away from any suitable juvenile habitat (Siegel et al. 2008), and are also subject to increased risk of starvation or predation throughout the highly vulnerable larval duration (Bailey and Houde 1989; Werner et al. 1996; Tanaka et al. 2008).

One species of significant scientific and economic interest with larval habitat that ranges from the open ocean to the coast is the American eel (*Anguilla rostrata*). This catadromous fish (living in freshwaters as an adult but spawning in the ocean) is found throughout the east coast of North America, but also as far south as Venezuela and as far north as southern Greenland (ASMFC 2012). The American eel is perhaps best known for its remarkable reproductive migrations: adults journey from their freshwater habitats all the way out to the Sargasso Sea in order to spawn (Schmidt 1923, 1931)—an uncommon behavior whereby all reproducing adults of the species gather in one location. American eel eggs and larvae have the potential to disperse from this open-ocean spawning site to habitats that span thousands of kilometers of coastline. Both adult fish and juvenile glass eels are harvested by commercial and sport fishers in many regions along the North American coast, particularly along the Gulf of Maine. Thus, the recent decline of American eel populations (Castonguay et al. 1994; Bonhommeau et al. 2008) has both ecological and economic implications.

American eel spawn in the Sargasso Sea from approximately February to April (McCleave et al. 1987; McCleave 2008), and larvae (termed leptocephali) then disperse from the region, with the successful individuals metamorphosing to the glass eel stage before reaching estuarine and freshwater coastal nursery habitats and ultimately making their way up rivers as well-developed juveniles. The leptocephalus larval phase lasts ~ 1 yr (Kleckner and McCleave 1985; McCleave 1993) and metamorphosis to the glass eel stage likely occurs over the continental slope or shelf (Kleckner and McCleave 1985). Glass eels enter estuaries or rivers, become pigmented, and after a poorly understood juvenile period of 3 to 30 yr (ASMFC 2012), eventually develop into adults, and complete the life cycle upon returning to the Sargasso Sea to spawn (Haro and Krueger 1988). Thus, in order to survive, the larvae must cross the Gulf Stream, the continental slope, and the shelf break jet and reach coastal freshwater nursery habitats within approximately their first year of life. What is known about the behavior of American eel larvae is limited, but they do exhibit diel vertical migrations from 30–70 m at night to 125–275 m during the day (Castonguay and

* Corresponding author: irypina@whoi.edu

McCleave 1987; Wuenschel and Able 2008). They are likely not very capable swimmers early in life, but are stronger swimmers later in their larval stage (Miller 2009), consistent with general findings that lateral swimming ability increases with larval ontogeny (Fisher et al. 2000). After metamorphosis, glass eels can reach, on average, short-term swimming speeds of up to 11.7–13.3 cm s^{-1} (Wuenschel and Able 2008).

The orientation of the major currents and topographic features that separate the Sargasso Sea from the U.S. east coast presents challenges to organisms attempting to traverse this domain. The dominant currents in this region, the Gulf Stream and the shelf break jet of the Middle Atlantic Bight, are directed along the coast, while the Gulf Stream extension flows northeastward, away from the coast. Thus, organisms attempting to swim towards the coast will tend to be swept along and/or away from the shore by the prevailing currents. Eddies, filaments, and meanders may assist an organism in its shoreward journey, but these motions are subject to dynamical constraints. For example, the Gulf Stream contains a potential vorticity gradient that is strongest in the shallowest 400 m and provides a potential restoring mechanism for the current (Yuan et al. 2004). The barrier effect is consistent with observations by Bower and Rossby (1989), who launched isopycnal floats within the Gulf Stream at different depths and found that only those launched below 400 m crossed from one side to the other. The barrier effect for the shallow Gulf Stream has also been well documented by others (Brambilla and Talley 2006; Burkholder and Lozier 2011; Rypina et al. 2011). Of course, the Gulf Stream path is occasionally broken by the formation of a warm-core or cold-core ring; the former could be particularly helpful in assisting an organism's motion towards the coast. An additional dynamical barrier is the shelf break jet that is, on average, aligned with the 100–200 m isobaths. A study of surface drifters released in this jet revealed a strong preference for downstream (i.e., along-isobath) advection with some offshore detrainment, but only minimal onshore detrainment (Lozier and Gawarkiewicz 2001). While eddies and filaments of offshore water are occasionally observed to make their way across the slope and onto the continental slope (Gawarkiewicz et al. 2001), one of the major questions about American eel larval migration is how larvae are able to reach their coastal destinations in the face of these strong, turbulent flows.

Interestingly, the American eel shares its spawning grounds with the European eel (*Anguilla anguilla*). The larvae of both species appear to take the same general routes out of the Sargasso Sea and become entrained in the Gulf Stream (McCleave and Kleckner 1987; McCleave 1993). However, the biological and behavioral mechanisms that cause American eel to reach North America, and European eel to reach Europe, are not well understood (McCleave 1993; Wang and Tzeng 2000; Tesch 2008). It is known that European eel have a longer larval period than American eel (Kleckner and McCleave 1985; McCleave 1993), giving them more time to reach their more distant juvenile habitats before metamorphosis. However, without behavioral differences between the two species, it seems likely that many European eel larvae would end up near the North American coast, and a great number of American eel larvae would be found en route toward Europe; neither scenario has been observed (McCleave 1993).

Although American eels have been the focus of several studies, many details of their larval journey, including the overall success rate of American eel larvae reaching North American coastal nursery habitats, and the importance of larval swimming speed and directionality in shaping dispersal patterns, remain mysteries. Here, we use a physical–biological numerical modeling approach, in which a model of ocean circulation is coupled with simple behavioral adaptations of larvae, to investigate aspects of American eel larval dispersal. We first examined the transport and spreading of larvae due to passive advection by realistic ocean currents (but including diel vertical migration). We then investigated larval dispersal pathways and success rates for a variety of different lateral swimming and navigation strategies, including simple nondirectional random walk–like swimming as well as directional swimming both with and without a preferred direction. We also investigated the variability in travel times from the Sargasso Sea to the coastal zone, defined to lie inshore of the 200 m isobath, as a function of latitude, and we studied the simulated distributions of larvae along the offshore edge of the North American coastal zone. Finally, model results for the successful larvae were used to identify the potential spawning locations within the Sargasso Sea that would maximize survival.

Methods

Larval pathways in this study are simulated from the output of the Family of Linked Atlantic Model Experiments (FLAME) ocean general circulation model (Böning et al. 2006; Biastoch et al. 2008). This model is configured with 45 z-coordinate vertical levels spaced from 10 m apart near the surface to 250 m at depth. The model has a horizontal resolution of 1/12°, and the domain is 100°W–16°E and 18°S–70°N. Following a 10 yr spin-up, the model was forced at the surface with time-varying air–sea fluxes constructed from two data sets. Specifically, monthly-averaged flux anomalies from the National Centers for Environmental Prediction and National Center for Atmospheric Research were superposed on European Center for Medium-Range Weather Forecasts monthly flux climatology. The FLAME model output spans 1990–2004 with a 3-d temporal resolution, but we only used a subset of these velocities covering 1995–1999 for the current study. The same model run has been used in a number of recent studies to investigate the subtropical to subpolar pathways in the North Atlantic (Burkholder and Lozier 2011), as well as the sources of eddy energy in the Labrador Sea (Eden and Böning 2002). The model is eddy permitting and exhibits realistic time-averaged and eddy fields.

The FLAME configuration was designed to address open-ocean questions rather than be used for coastal applications, so its ability to realistically represent coastal currents is not well established. Although the model qualitatively reproduces some of the prominent features

of the circulation in the Mid- and South Atlantic Bights, its relatively coarse resolution and absence of freshwater coastal sources and tides present drawbacks for tracking larval trajectories in coastal regions. Thus, we focused here primarily on larval transport from the Sargasso Sea to the shelf break, defined here as the 200 m isobath. Though we have followed trajectories inshore of the 200 m isobath for the purpose of illustration, we note that the inshore path segments are less reliable than the offshore portions.

In order to account for the diel vertical migration of eel larvae in our model, simulated larval particles were advected with the depth-averaged currents between 25 m and 76 m at night and between 124 m and 290 m during the day. These depth levels in FLAME are closest to the diel vertical migration depths (30–70 m at night to 125–275 m at day) reported in the literature (Castonguay and McCleave 1987; Wuenschel and Able 2008). The actual depth of a particular organism at a particular time is not estimated since this would require knowledge of the vertical speed of the organism relative to the fluid. Instead, we tracked the horizontal motion of the organism by assuming that it reaches the upper nighttime layer at midnight and the deeper daytime layer at noon, spending 12 h in steady ascent and descent between the layers for a total of 24 h. In simulations with actively swimming larvae, horizontal velocities of prescribed amplitude and direction were superposed on the ocean currents. In all simulations, except those with the random walk swimming strategy (*see* below), larval trajectories were computed using a variable-step 4th-order Runge–Kutta integration scheme with the bilinear velocity interpolation in time and space between the grid points. In the random walk simulations, a fixed-step 4th-order Runge–Kutta integration scheme was employed. In all simulations larvae were released once per day during the spawning season in February–April in years 1995 through 1999, and larval trajectories were tracked for 1 yr. Similar to Bonhommeau et al. (2009), larvae were released on a regular grid inside a rectangular domain from 74°W to 55°W and from 22°N to 30°N, corresponding to what is commonly considered to be the general spawning area of American eel in the Sargasso Sea (Kleckner and McCleave 1985; McCleave et al. 1987).

Laboratory studies have suggested that glass eels (the stage at which they enter estuaries) can swim, on average, at speeds up to 12–13 cm s^{-1}, and that long-term swimming speeds are roughly half these maximum values, or about 6–6.5 cm s^{-1} (Wuenschel and Able 2008). In order to account for these characteristics, we allowed the swimming speed of simulated eel larvae to increase linearly with age from 0 cm s^{-1} at the time of hatching to a value of U_{1yr} at the end of the development stage. We vary the final speed U_{1yr} from zero to 10 cm s^{-1} and, following Kleckner and McCleave (1985) and McCleave (1993), set the time of larval transition to glass eel stage to be 12 months.

It is not known whether American eel larvae can orient themselves in the ocean and maintain their direction. We therefore explored four different lateral swimming scenarios. The first scenario tested whether larvae can simply rely on ocean currents to bring them from the spawning grounds to shelf and coastal areas along the east coast of the U.S. For this test, we released simulated larvae in the Sargasso Sea, accounting for their diel vertical migration, but did not implement any horizontal swimming ability. The second scenario employed random walk horizontal swimming—the simplest navigation behavior we could envision. This strategy does not require an eel larva to know its location or orientation but simply represents a behavior where swimming direction is randomly changed. The alternative to random walk swimming is directional swimming, where a larva can sense its direction with respect to some cue and thus maintain its heading. This hypothesis was explored in scenarios 3 and 4. For the third scenario—directional swimming with equally likely chosen directions—we randomly assigned each simulated larva an initial swimming direction that it maintained for its entire lifetime. Dependencies on the larval swimming speed and direction were explored by varying U_{1yr} from 2 cm s^{-1} to 10 cm s^{-1} and swimming direction from 0° to 360°. Finally, the fourth swimming scenario tested directional swimming with a preferred direction, where larvae swam primarily northwestward (towards the northeast U.S. coast). Numerical runs for scenarios 1 and 2 were based on 1 million particles; scenarios 3 and 4 utilized 5 million particles.

Model simulations with passively advected larvae and random walk swimming of larvae (scenarios 1 and 2) did not incorporate larval mortality, but our investigations of scenarios 3 and 4 did. Though larval mortality in the open ocean is challenging to measure, it is possible to estimate assuming an equal-gender steady-state adult fish population, where each adult female produces two surviving individuals. Bonhommeau et al. (2009) used this approach to estimate mortality of European eel. Since European and American eels are similar species (and congeners) that spawn in the same location and travel through the same waters during the first year of their development, they are likely to be exposed to the same predators and same food availability. With this in mind, we use a mortality rate (i.e., exponential decay) of $M = 3.8\ yr^{-1}$ from Bonhommeau et al. (2009), which results in roughly 2% of the larvae surviving after 1 yr.

Results

Scenario 1: Dispersal of passively advected larvae—We estimated the probability of passively advected simulated larvae released in the Sargasso Sea reaching each geographical location in the western North Atlantic, including the shelf and coastal areas inshore of the 200 m isobath (Fig. 1a). In this calculation, simulated larvae were released in the spawning domain (dashed rectangle in Fig. 1a) and their trajectories were computed as described in the Methods section. The North Atlantic was then divided into $(1:12)^\circ \times (1:12)^\circ$ bins, and the probability to visit each bin was estimated by dividing the number of trajectories that pass through a bin by the total number of released larvae. Note that we are counting the number of larvae visiting each bin, not the number of bin visits, so even if a larva visits the same bin more than once, it is still counted as one visit. The probabilities shown do not

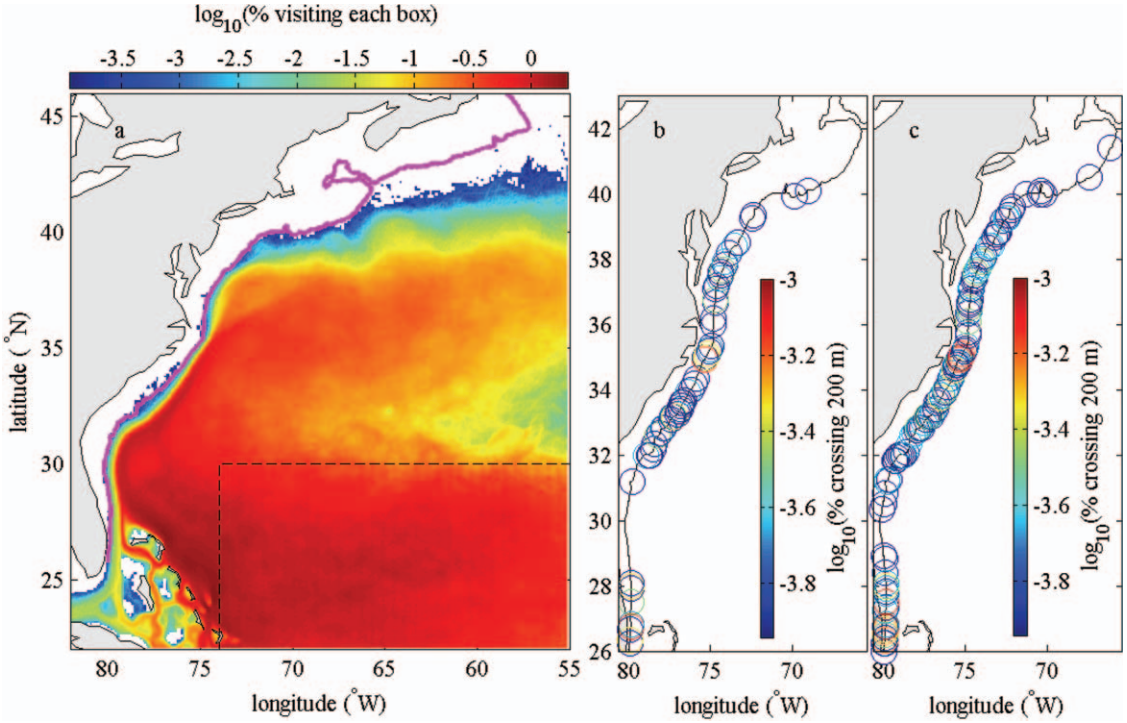

Fig. 1. (a) Probability for passively advected simulated larvae released in the Sargasso Sea (dashed box) during the spawning season to visit different geographical locations in the North Atlantic. Simulation includes diel vertical migration and covers 1995–1999 with trajectory integration of 1 yr. Probability is shown by color on a logarithmic scale, white corresponds to zero probability. Magenta shows the 200 m isobath, land is shaded in gray. (b) In the same simulation, the probability to cross the 200 m isobath (black curve). (c) Same as Fig. 1b but in simulations with random walk swimming strategy with 3 h time interval between successive direction changes.

include larval mortality, and though we track trajectories onto the shelf, probabilities computed for the region lying inshore of the 200 m isobath may be unreliable. We are primarily interested in whether the trajectories can get to the shelf.

Consistent with expectations based on the mean flow in the subtropical gyre and Gulf Stream, larvae were advected from the spawning region to the west and northwest, many making their way into the Gulf Stream and/or Gulf Stream extension, either of which must be crossed in order to reach shelf and coastal waters. The results also reveal several southern pathways through the Bahamas and into the Florida Straits. A much smaller percentage enters the Gulf Stream via the Loop Current. Of note is the very sharp decrease in probability across the Gulf Stream and the low probabilities along the inshore coastal regions and in some places offshore of the 200 m isobath (shown by the magenta curve in Fig. 1a). This map indicates that it is extremely unlikely for passively advected eel larvae to cross the 200 m isobath and reach shelf and coastal waters by simply riding the oceanic currents and changing depth diurnally. Specifically, even without accounting for larval mortality, only about 0.014% of larvae in this scenario make it to the coastal zone. The probability distribution was further examined spatially by calculating the probability for eel larvae to cross the 200 m isobath at different geographical locations (Fig. 1b). Probabilities to cross the 200 m isobaths are very small, the distribution is patchy, and, notably, there are no trajectories crossing the 200 m isobath north of 40°N. While we cannot definitively say that passive drift is not adequate for population replenishment, we clearly show below that directional swimming substantially improves the chances of survival for American eel larvae.

From a physical oceanographic point of view, these results are not surprising since the Gulf Stream, the continental slope, and the shelf break are all potential impediments to transport (Lozier and Gawarkiewicz 2001; Rypina et al. 2011). However, from a larval recruitment point of view, these results suggest that larval swimming is likely required in order to sustain the population in coastal waters. Moreover, without active swimming, simulated larvae in our model do not reach the Gulf of Maine, where ingressing American eel (elvers) are typically abundant and actively harvested each year.

Scenario 2: Random walk swimming—To identify factors that may significantly raise the likelihood of American eel larvae reaching coastal waters, we investigated scenarios that prescribe a variety of active larval swimming behaviors. For the random walk swimming scenario, larvae were allowed to swim and to change directions in a random manner. This behavior could apply if larvae are able to swim but not sense direction. The time interval (Δt) over which an organism could or would maintain its direction is unknown, so we performed separate calculations for Δt = 30 min, 3 h, and 24 h. Each simulation was based on 1 million simulated larvae with a swimming speed reaching

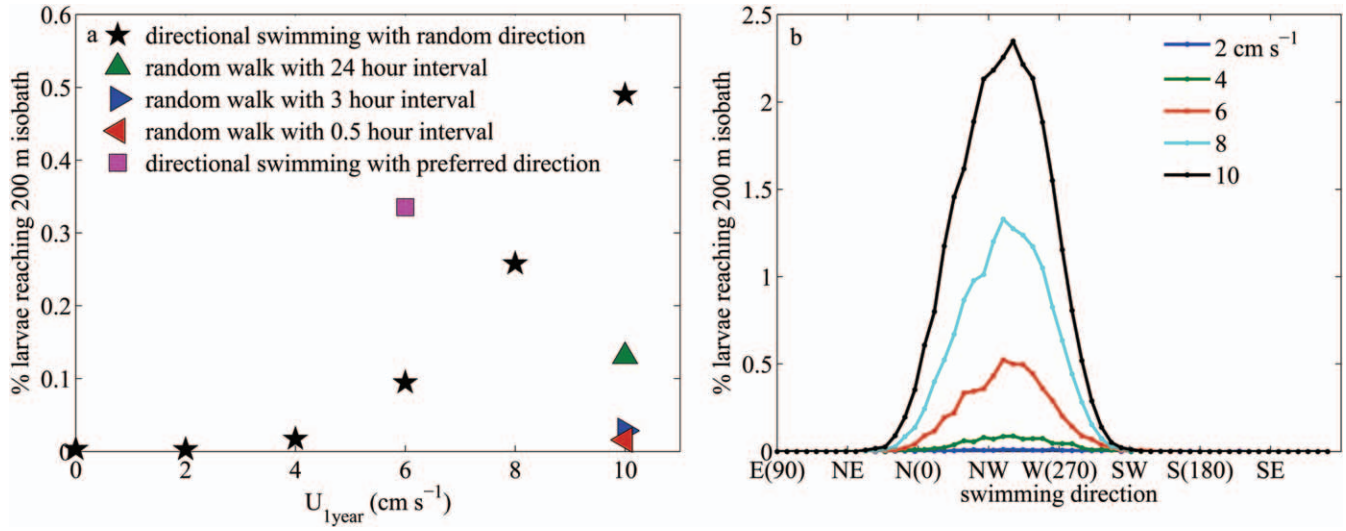

Fig. 2. (a) Success rate (in percent) of simulated larvae crossing the 200 m isobath for different swimming strategies and different swimming speeds. Each model run covered 1995–1999 and was based on ≥1 million simulated particles released in the Sargasso Sea in February–April of each year. Directional swimming simulations included mortality (at $M = 3.8\ \mathrm{yr}^{-1}$); random walk simulations did not include mortality. (b) For directional swimming simulations with random direction (corresponding to black stars in (a)), probability to cross the 200 m isobath as a function of swimming direction for different swimming speeds U_{1yr}. In this model run, we randomly assigned the larvae an initial direction and then had them maintain it for the entire journey.

$U_{1yr} = 10\ \mathrm{cm\ s}^{-1}$ at the end of 12 months (> 1.5 times the observed value). Thus, the simulated organisms swim at a speed that increases linearly in time from zero to U_{1yr} and change direction randomly at the end of each time interval Δt. The total velocity (in vector components) of an individual organism at each point in time is the sum of the imposed swimming velocity and the ocean model horizontal fluid velocity at the location of the particle.

Generally, for a given swimming speed, a larger time interval between direction changes increases the deviation of the randomly swimming larva from its passive drift path, thus leading to larger probabilities of reaching the shelf. To understand this effect, consider a random walk of N steps of length X in a random direction. The root-mean-square (rms) distance from the initial location is given by $d_{rms} = X \times N^{1/2}$. We use $X = v\Delta t$ and $N = T/\Delta t$, where v is larval swimming velocity and T is trajectory integration time. Thus, the rms distance increases with increasing Δt according to $d_{rms} = v\Delta t^{1/2}T^{1/2}$, so that longer time intervals lead to larger deviations from the passive-drift path and generally increase the chance of eel larvae reaching coastal waters. This effect was confirmed in our numerical simulations: the probability of successfully crossing the 200 m isobath increased from 0.016% for $\Delta t = 30$ min to 0.029% for $\Delta t = 3$ h to 0.13% for $\Delta t = 24$ h (colored triangles in Fig. 2a), without mortality being incorporated. The probability of crossing the 200 m isobath (Fig. 1c) remains patchy (although less so than for the passively drifting larvae) and again, virtually equal to zero north of 40°N. Out of 1 million particles released, only four crossed the 200 m isobath north of 40°N, and this number does not account for mortality.

Scenario 3: Directional swimming with equally likely chosen directions—It is also possible that larvae can maintain a compass direction while swimming, but lack the ability to orient toward a particular preferred destination. A plausible strategy consistent with this constraint is one in which the larvae choose a direction randomly and then maintain that direction during their entire journey. This strategy is equivalent to scenario 2 with $\Delta t \to \infty$, and we refer to it as directional swimming. We also accounted for larval mortality by using a mortality rate (or exponential decay) of $M = 3.8\ \mathrm{yr}^{-1}$ as in Bonhommeau et al. (2009). As indicated by the black stars in Fig. 2a, implementation of the directional swimming strategy led to a substantial increase in the percentage of larvae reaching the coastal zone. The probability of crossing the 200 m isobath (shown in Fig. 2a) varies from 0.003% at $U_{1yr} = 2\ \mathrm{cm\ s}^{-1}$ to 0.5% for $U_{1yr} = 10\ \mathrm{cm\ s}^{-1}$ after accounting for larval mortality, compared to $\sim 3 \times 10^{-4}$% for passively drifting larvae with mortality included or, equivalently, 0.014% without larval mortality. As expected, the probability to reach the coastal zone increased monotonically with increasing swimming speed; however, the rate of this increase was slower for $U_{1yr} \le 4\ \mathrm{cm\ s}^{-1}$and faster for $U_{1yr} \ge 6\ \mathrm{cm\ s}^{-1}$, which roughly corresponds to the average swimming speed of ingressing glass eels (Wuenschel and Able 2008). Whereas for slow larvae, the increase in swimming speed from 0 cm s^{-1} to 2 or 4 cm s^{-1} led to only a relatively small increase in the probability, eel larvae with a slightly better than average swimming ability have a much better chance of survival.

Examining swimming directions with the likelihood of crossing the 200 m isobath, larvae that swam from the Sargasso Sea toward the coast (i.e., at a compass heading of ~ 300°) had the highest probability of reaching coastal waters (Fig. 2b). The dependence on swimming direction was approximately Gaussian, and the optimal swimming direction was almost independent of swimming speed.

Scenario 4: Directional swimming with a preferred swimming direction—Not surprisingly, simulations with unbiased directional swimming (Scenario 3) indicated that it is advantageous for American eel larvae to swim to the northwest from their spawning location. It has been hypothesized (Kleckner and McCleave 1985; Miller 2009; Righton et al. 2012) that American eel larvae have evolved to orient in a particular direction to optimize their chance of survival (i.e., by reaching coastal habitats). This hypothesis was investigated in the fourth swimming scenario, where instead of assigning each larva a random swimming direction, we implemented a Gaussian distribution of directions with the parameters (mean and standard deviation [SD]) fit to give the best agreement with the curves in Fig. 2b.

For the most realistic maximum swimming speed of $U_{1yr} \approx 6$ cm s^{-1}, the preferred swimming direction strategy led to an $\sim$ 3.5-fold increase in the success rate (purple square in Fig. 2a) compared to directional swimming with an equally likely chosen direction ($\sim$ 0.34% vs. $\sim$ 0.1%, respectively). The magnitude of this increase can be anticipated by writing down the success rate as $P = \int_0^{2\pi} N(\alpha) f(\alpha) d\alpha$, where α is the swimming direction, $N(\alpha)$ is the particle density distribution of the simulated larvae in direction α, and $f(\alpha)$ is the probability density function of larval success rates in direction α, which in our case is simply Gaussian, $f(\alpha) = f_0 e^{-(\frac{\alpha-\mu}{\sigma})^2}$. Further progress can be made by writing down the particle density distributions for simulations without and with the preferred direction, respectively, as $N_{\text{uniform}}(\alpha) = N_{\text{tot}}/2\pi$ and $N_{\text{preferred}}(a) = \left[N_{\text{tot}} \Big/ \left(\int_0^{2\pi} e^{-(\frac{\alpha-\mu}{\sigma})^2} d\alpha \right) \right] e^{-(\frac{\alpha-\mu}{\sigma})^2}$, where the total number of released simulated larvae, N_{tot}, is the same in both simulations. Plugging these formulas back into the expression for P, we obtain $P_{\text{preferred}}/P_{\text{uniform}} = 2\pi \int_0^{2\pi} e^{-(\frac{\alpha-\mu}{\sigma})^2} d\alpha \Big/ \left(\int_0^{2\pi} e^{-(\frac{\alpha-\mu}{\sigma})^2} d\alpha \right)^2 \cong 3.5$ for μ and σ estimated numerically to give the best agreement with the curves in Fig. 2b.

Dispersal pathways, travel times, and success rates of American eel larvae under scenario 4—As shown in Fig. 3, a number of larval dispersal pathways connect the Sargasso Sea spawning area to the coastal waters. The major and most direct pathway carried larvae to the northwest from the Sargasso Sea, with subsequent entrainment into the eastern flank of the Gulf Stream and detrainment from its western side. Secondary pathways took larvae through the Bahamas to the Florida Current or along the northern coast of Cuba through Old Bahama Channel and then into the Florida Current either via the Nicholas or Santaren Channels. Active swimming substantially enhanced detrainment from the Gulf Stream's western and northern flank and transport across the slope and shelf break. As indicated by the Fig. 3 inset, spawning success (i.e., probability of larvae released at a given geographical location reaching coastal environments in 1 yr) within the Sargasso Sea increased generally from east to west, reaching the largest values near the southwestern corner of the release domain. In this calculation the spawning box was divided into $0.75^\circ \times 0.5^\circ$ bins, and the spawning success in each bin was estimated by dividing the number of successful simulated larvae released in a bin by the total number of simulated larvae released in that bin. The distribution of successful larvae along the 200 m isobath (Fig. 4a,b) showed nonzero probabilities along most of the North American coast, including the latitudes of the Gulf of Maine, where American eel elvers are harvested each year, as well as areas farther north. This pattern was in sharp contrast to the extremely weak and patchy distributions for larvae with no swimming ability and for those with random walk–like swimming (Fig. 1b,c). Our model suggests that it takes $\sim$ 280–320 d for larvae swimming to the northwest to cross the 200 m isobath (Fig. 4c,d) and an additional 1–2 months to cross the shelf and reach the coast; however, a higher-resolution and dedicated coastal circulation model would be required to confirm this latter time estimate. Mean travel times generally increase with latitude, and this variation is on the order of a month. Interestingly, predicted travel times of $\sim$ 1 yr are consistent with the time between hatching and estuarine ingress by glass eels (Kleckner and McCleave 1985; Sullivan et al. 2006; McCleave 2008).

With the estimated travel times (Fig. 4c,d), we quantified the sensitivity of our results to the mortality rate. Using the average travel time of 1 yr, a 10% increase (decrease) in the *M*-value leads to about 30% decrease (46% increase) in the percentages of surviving larvae after 1 yr. Note, however, that because of the slight increase in travel time with latitude, larvae reaching coastal waters farther north (e.g., in the Gulf of Maine) would be slightly more sensitive to the increased mortality value than larvae reaching the southern parts of the Mid-Atlantic Bight.

Discussion

The horizontal swimming and navigation strategy of American eel larvae is essentially unknown, and there is debate as to whether swimming is critical for recruitment of European eel (McCleave et al. 1998) and whether it serves as the mechanism by which American and European eels reach their respective coastal habitats (McCleave 1993; Wang and Tzeng 2000; Tesch 2008). We used a coupled biological–physical model, which melds taxon-specific characteristics and behaviors with a high-resolution ocean general circulation model, to study the larval dispersal pathways and success rates of American eel larvae, including the influence of swimming speeds and navigation strategies. We tested a variety of swimming behaviors—passive drift, random walk swimming, and directional navigation with and without a preferred swimming direction—in order to explore which strategies significantly increase the number of American eel larvae reaching coastal nursery habitats.

Our analyses suggest that passive drift and random walk swimming yield extremely small percentages of successful larvae. Though a paucity of data prevents us from concluding that such percentages are too small for population replenishment, we showed that directional swimming of larvae improves the chances of survival for American eel larvae by three orders of magnitude compared to the passive drift scenario. Our results also

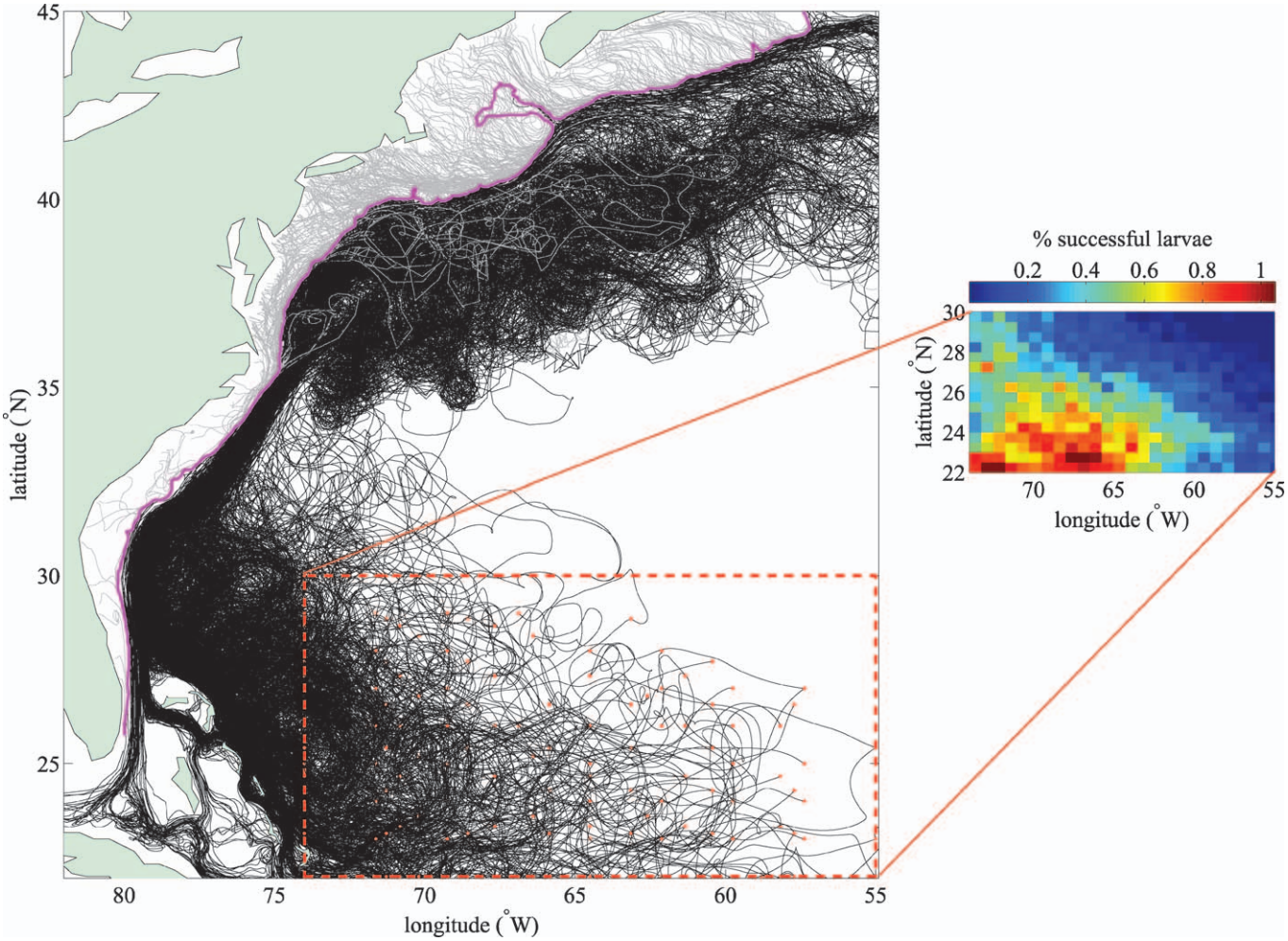

Fig. 3. A subset of successful larval trajectories reaching the 200 m isobath from a coupled physical–biological model for American eel larvae. The simulation covered 1995–1999, was based on 5 million simulated particles, and included diel vertical migration, directional swimming with a Gaussian distribution of angles (i.e., directional swimming with preferred direction corresponding to the purple square in Fig. 2a), swimming speed increasing linearly from 0 to $U_{1yr} = 6$ cm s^{-1} over 1 yr, and mortality rate of $M = 3.8$ yr^{-1}. Black shows larval tracks from the deployment location to the first crossing of the 200 m isobath, with gray tracks after the first crossing. Land is shown in green, the 200 m isobath is shown in magenta, and the deployment box is shown in red. The small inset shows probability (in %) of successful larvae as a function of larval deployment location within the deployment box. We remind the reader that the path segments inshore of 200 m (shown in gray) are less reliable than their offshore portions. These nearshore path segments are not used for quantifying the success rates and travel times in Figs. 2 and 4.

indicate that swimming primarily to the northwest from the spawning area in the Sargasso Sea roughly tripled the success rate of American eel larvae compared to the scenario without a preferred swimming direction. Moreover, unlike passive drift and random walk scenarios, directional swimming also leads to successful larvae reaching the coastal areas along most of the North American coast, including the Gulf of Maine, where American eel elvers are known to be abundant.

Directional swimming has been observed in larvae of several fish species (Leis et al. 1996; Stobutzki and Bellwood 1998; Leis and Carson-Ewart 2003). The ability for a larva to maintain its heading implies that it can sense direction and thus orient with respect to some cue. While orientation to near-coastal cues via hearing and olfaction has been shown (Atema et al. 2002; Montgomery et al. 2006), the use of navigational cues for orientation in the open ocean has been difficult to prove. It could be hypothesized that eel larvae might navigate using gradients in the physical characteristics of seawater such as temperature or salinity. Indeed, while there is support that glass eels may use freshwater signals from river mouths for recruitment to estuaries (i.e., where gradients are large over small spatial scales; Sullivan et al. 2006), navigation by such mechanisms seems less feasible in the open ocean where gradients are much weaker and extend over tens to hundreds of kilometers. Small, slow-swimming larvae would need to ''remember'' conditions that occurred perhaps days to weeks prior in order to navigate by chemical gradients. Furthermore, larvae entrained in a

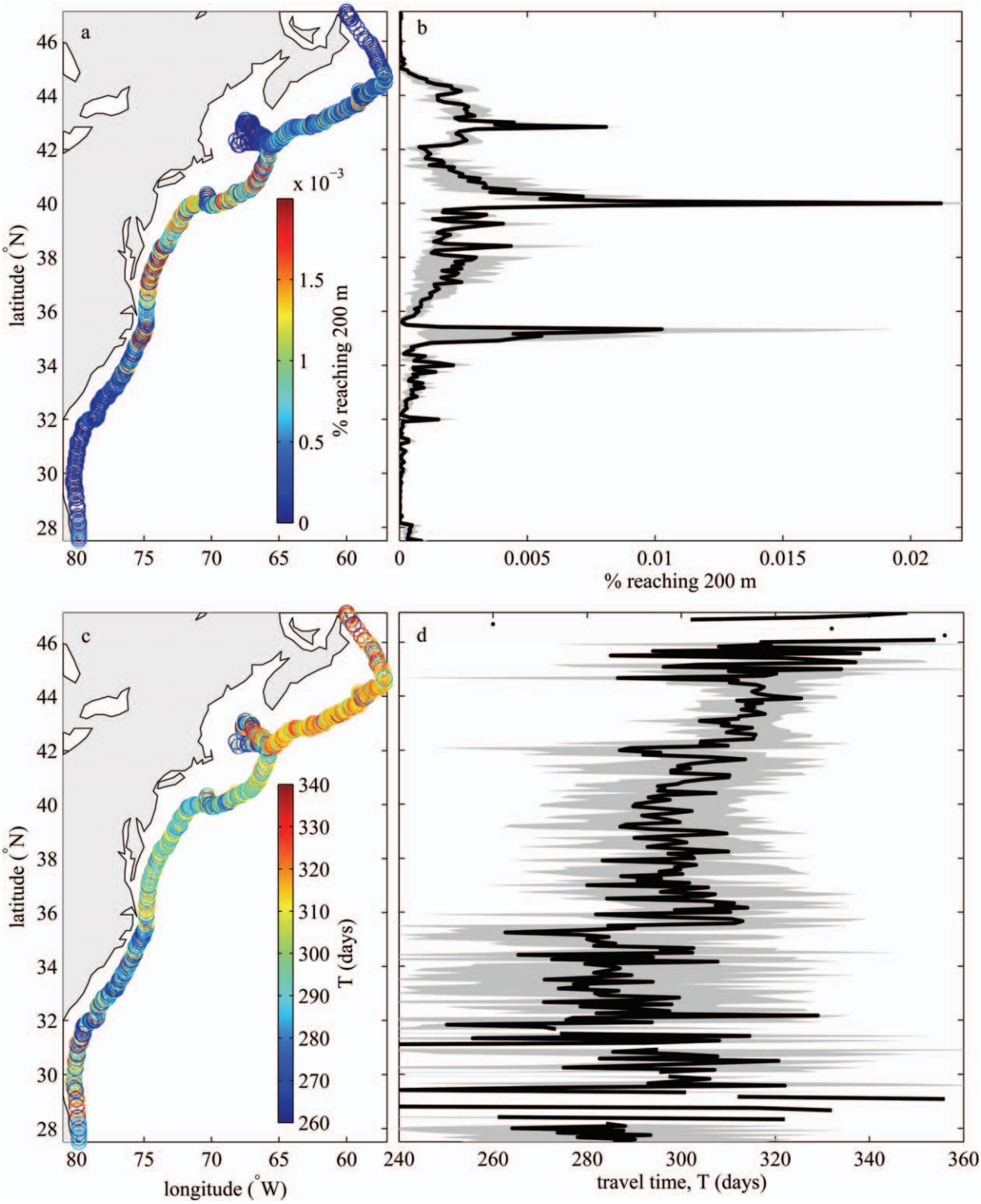

Fig. 4. Results from a coupled physical–biological model with diel vertical migration, directional swimming with a Gaussian distribution of angles, swimming speed increasing linearly from 0 to 6 cm s^{-1} over 1 yr, and mortality rate of $M = 3.8$ yr^{-1}. Simulation included 5 million particles released in the Sargasso Sea during the spawning season in years 1995 to 1999. (a) Probability to cross the 200 m isobath. (b) Probability to cross the 200 m isobath as a function of latitude. (c) Travel time map: ensemble-averaged travel times from the spawning area to the 200 m isobath. (d) Travel time to the 200 m isobath as a function of latitude. (b,c) Black curve shows the mean and gray corresponds to the 1 SD interval.

parcel of water and unable to view the ocean bottom are unlikely to sense—and, thus, navigate—using ocean currents or bathymetry. One cue that eel and other fish larvae could potentially use in oceanic waters to orient and swim directionally is geomagnetism or similar cues such as celestial bodies or polarized light (Mouritsen et al. 2013). There is substantial support in the literature on the use of geomagnetic information for orientation (Wiltschko and Wiltschko 1995; Lohmann et al. 2007), and this ability has been observed in all major groups of animals (even bacteria), including adult eels (Tesch et al. 1992; Durif et al. 2013) and the larvae of sockeye salmon (*Oncorhynchus nerka*) and brown trout (*Salmo trutta*) (Formicki et al. 2004). Although the ability of eel larvae to sense and use magnetic fields or similar cues has not been proven, if such an ability existed, it would allow larvae in the open ocean to maintain their swimming direction for extended periods of time and, as clearly indicated in our modeling study, would significantly improve the success rates of American eel larvae reaching coastal waters.

Our model suggests that within the general area of the Sargasso Sea, the most probable spawning locations of American eel lie in the southwestern part of the domain (indicated by the red colors in the inset of Fig. 3). Remarkably, this is in qualitative agreement with the empirical larval distribution data of Kleckner and McCleave (1985; *see* their fig. 2) who found the smallest (i.e., youngest) larvae ($<$ 10 mm) in this same geographical region. Additionally, since our high-survival spawning area is smaller than those generated by previous larval survey methods, our results may help zero in on the precise spawning location of American eel, which is still not known.

Our estimated success rates are sensitive to the (unknown) mortality rate for American eel larvae. The mortality rate $M = 3.8\ \mathrm{yr}^{-1}$ for European eel larvae is the best estimate available and our use of it comes with a caveat. In the method used by Bonhommeau et al. (2009), M is based on the percentage of larvae that do not reach Europe as glass eels. This group includes larvae that die before they reach the glass eel stage and also larvae that reach the glass eel stage at a location sufficiently remote that they cannot reach Europe alive. In our simulations, this second group is accounted for independently. It consists of trajectories that do not cross our finish line (the 200 m isobath) by the end of the defined 1-yr larval stage. Therefore, our mortality rate should reflect only the continuous death rate of larvae over our 1-yr integration period, so the value of M we have used may prove to be an overestimate. Should improved mortality estimates become available, the success rates reported here could be recalculated by rescaling with a new M, as described at the end of the Results section.

In summary, results from our analyses highlight specific behavioral adaptations that could allow American eel larvae to improve their chances of survival, strongly supporting the likelihood that some degree of directional, horizontal swimming capability is required for larvae to reach coastal nursery habitats. For the four swimming behaviors considered—passive drift, random walk swimming (with $U_{1yr} = 10\ \mathrm{cm\ s}^{-1}$ and $\Delta t = 3$ h), directional navigation (with $U_{1yr} = 6\ \mathrm{cm\ s}^{-1}$) without and with a preferred (northwestern) swimming direction—the success rates of American eel larvae in our model reaching the shelf were roughly $3 \times 10^{-4}\%$, $6.5 \times 10^{-4}\%$, 0.1%, and 0.34%, respectively, after accounting for larval mortality. Also, simulated larvae with swimming abilities even slightly above estimated average values ($\sim 6\ \mathrm{cm\ s}^{-1}$ at the end of the 1 yr developmental time) have a much better chance of survival compared to slow-swimming larvae. Supporting the utility of our model, the transit time scale of about 1 yr for simulated larvae to reach the coast is in agreement with field-based observations. Finally, within the considered spawning box, a portion of the southwestern Sargasso Sea was identified as the most probable spawning area.

Future work could focus on investigating the causes and consequences of the American eel population decline, the possible differences in behavioral adaptations between the American and European eels, and the pathways taken by larval and glass eels over the continental shelf. In addition, it will be important to describe in more detail the physical oceanographic features (eddies, Gulf Stream rings, filaments, etc.) that enhance or retard the transport of larvae towards coastal habitats. Sub-mesoscale features not resolved by FLAME, or suppressed by our vertical averaging, may play a role.

Acknowledgments

I.I.R. and L.J.P. were supported by grant 85464100 from the National Science Foundation. Support for J.K.L. came from the Woods Hole Oceanographic Institution Penzance Endowed Support for Assistant Scientists. M.S.L. was supported by grant Ocean-Sciences-0960776 from the National Science Foundation. We thank M. Hauff for reviewing and improving earlier manuscript drafts, and two anonymous reviewers for their improvements of this manuscript.

References

Atema, J., M. J. Kingsford, and G. Gerlach. 2002. Larval reef fish could use odour for detection, retention and orientation to reefs. Mar. Ecol. Prog. Ser. **241:** 151–160, doi:10.3354/meps241151

Atlantic States Marine Fisheries Commission (ASMFC). 2012. American eel benchmark stock assessment [Internet]. ASMFC Stock Assessment 12-01. Raleigh (NC): Atlantic States Marine Fisheries Commission [accessed 20 March 2013]. Available from http://www.asmfc.org/species/american-eel

Bailey, K. M., and E. D. Houde. 1989. Predation on eggs and larvae of marine fishes and the recruitment problem. Adv. Mar. Biol. **25:** 1–83, doi:10.1016/S0065-2881(08)60187-X

Biastoch, A., C. W. Böning, J. Getzlaff, J.-M. Molines, and G. Madec. 2008. Causes of interannual-decadal variability in the meridional overturning circulation of the midlatitude North Atlantic Ocean. J. Clim. **21:** 6599–6615, doi:10.1175/2008JCLI2404.1

Bonhommeau, S., E. Chassot, B. Planque, E. Rivot, A. H. Knap, and O. Le Pape. 2008. Impact of climate on eel populations of the Northern Hemisphere. Mar. Ecol. Prog. Ser. **373:** 71–80, doi:10.3354/meps07696

———, and others. 2009. Estimates of the mortality and the duration of the trans-Atlantic migration of European eel *Anguilla anguilla* leptocephali using a particle tracking model. J. Fish Biol. **74:** 1891–1914, doi:10.1111/j.1095-8649.2009.02298.x

Böning, C. W., M. Scheinert, J. Dengg, A. Biastoch, and A. Funk. 2006. Decadal variability of subpolar gyre transport and its reverberation in the North Atlantic overturning. Geophys. Res. Lett. **33:** L21S01, doi:10.1029/2006GL026906

Bower, A., and T. Rossby. 1989. Evidence of cross-frontal exchange processes in the Gulf Stream based on isopycnal RAFOS float data. J. Phys. Oceanogr. **19:** 1177–1190, doi:10.1175/1520-0485(1989)019<1177:EOCFEP>2.0.CO;2

Brambilla, E., and L. D. Talley. 2006. Surface drifter exchange between the North Atlantic subtropical and subpolar gyres. J. Geophys. Res. **111:** C07026, doi:10.1029/2005JC003146

Burkholder, K. C., and M. S. Lozier. 2011. Subtropical to subpolar pathways in the North Atlantic: Deductions from Lagrangian trajectories. J. Geophys. Res. **116:** C07017, doi:10.1029/2010JC006697

Castonguay, M., P. Hodson, C. Couillard, M. Eckersley, J.-D. Dutil, and G. Verreault. 1994. Why is recruitment of the American eel, *Anguilla rostrata*, declining in the St. Lawrence River and Gulf? Can. J. Fish. Aquat. Sci. **51:** 479–488, doi:10.1139/f94-050

———, and J. D. McCleave. 1987. Vertical distributions, diel and ontogenetic vertical migrations and net avoidance of leptocephali of *Anguilla* and other common species in the Sargasso Sea. J. Plankton Res. **9:** 195–214, doi:10.1093/plankt/9.1.195

Cowen, R. K., and S. Sponaugle. 2009. Larval dispersal and marine population connectivity. Annu. Rev. Mar. Sci. **1:** 443–466, doi:10.1146/annurev.marine.010908.163757

Durif, C. M. F., H. I. Browman, J. B. Phillips, A. B. Skiftesvik, L. A. Vollestad, and H. H. Stockhausen. 2013. Magnetic compass orientation of the European eel. PLoS One **8:** e59212, doi:10.1371/journal.pone.0059212

Eden, C., and C. Böning. 2002. Sources of eddy kinetic energy in the Labrador Sea. J. Phys. Oceanogr. **32:** 3346–3363, doi:10.1175/1520-0485(2002)032<3346:SOEKEI>2.0.CO;2

Epifanio, C. E., and R. W. Garvine. 2001. Larval transport on the Atlantic continental shelf of North America: A review. Estuar. Coast. Shelf Sci. **52:** 51–77, doi:10.1006/ecss.2000.0727

Fisher, R., D. R. Bellwood, and S. Job. 2000. Development of swimming abilities in reef fish larvae. Mar. Ecol. Prog. Ser. **202:** 163–173, doi:10.3354/meps202163

Formicki, K., M. Sadowski, A. Tański, A. Korzelecka-Orkisz, and A. Winnicki. 2004. Behaviour of trout (*Salmo trutta* L.) larvae and fry in a constant magnetic field. J. Appl. Ichthyol. **20:** 290–294, doi:10.1111/j.1439-0426.2004.00556.x

Gawarkiewicz, G., F. Bahr, R. C. Beardsley, and K. H. Brink. 2001. Interaction of a slope eddy with the shelfbreak front in the Middle Atlantic Bight. J. Phys. Oceanogr. **31:** 2783–2796, doi:10.1175/1520-0485(2001)031<2783:IOASEW>2.0.CO;2

Hare, J. A., and others. 2002. Routes and rates of larval fish transport from the southeast to the northeast United States continental shelf. Limnol. Oceanogr. **47:** 1774–1789, doi:10.4319/lo.2002.47.6.1774

Haro, A. J., and W. H. Krueger. 1988. Pigmentation, size, and migration of elvers (*Anguilla rostrata* (Lesueur)) in a coastal Rhode Island stream. Can. J. Zool. **66:** 2528–2533, doi:10.1139/z88-375

Kleckner, R., and J. McCleave. 1985. Spatial and temporal distribution of American eel larvae in relation to North Atlantic Ocean current systems. Dana **4:** 67–92.

Leis, J. M., and B. M. Carson-Ewart. 2003. Orientation of pelagic larvae of coral-reef fishes in the ocean. Mar. Ecol. Prog. Ser. **252:** 239–253, doi:10.3354/meps252239

———, H. P. Sweatman, and S. E. Reader. 1996. What the pelagic stages of coral reef fishes are doing out in blue water: Daytime field observations of larval behavioural capabilities. Mar. Freshw. Res. **47:** 401–411, doi:10.1071/MF9960401

Levin, L. A. 2006. Recent progress in understanding larval dispersal: New directions and digressions. Integr. Comp. Biol. **46:** 282–297, doi:10.1093/icb/icj024

Lohmann, K. J., C. M. Lohmann, and N. F. Putman. 2007. Magnetic maps in animals: Nature's GPS. J. Exp. Biol. **210:** 3697–3705, doi:10.1242/jeb.001313

Lozier, M. S., and G. Gawarkiewicz. 2001. Cross-frontal exchange in the Middle Atlantic Bight as evidenced by surface drifters. J. Phys. Oceanogr. **31:** 2498–2510, doi:10.1175/1520-0485(2001)031<2498:CFEITM>2.0.CO;2

McCleave, J. 1993. Physical and behavioural controls on the oceanic distribution and migration of leptocephali. J. Fish Biol. **43:** 243–273, doi:10.1111/j.1095-8649.1993.tb01191.x

McCleave, J. D. 2008. Contrasts between spawning times of *Anguilla* species estimated from larval sampling at sea and from otolith analysis of recruiting glass eels. Mar. Biol. **155:** 249–262, doi:10.1007/s00227-008-1026-8

———, P. J. Brickley, K. M. O'Brien, D. A. Kistner, M. W. Wong, M. Gallagher, and S. M. Watson. 1998. Do leptocephali of the European eel swim to reach continental waters? Status of the question. J. Mar. Biol. Assoc. UK **78:** 285–306, doi:10.1017/S0025315400040091

———, and R. C. Kleckner. 1987. Distribution of leptocephali of the catadromous *Anguilla* species in the western Sargasso Sea in relation to water circulation and migration. Bull. Mar. Sci. **41:** 789–806.

———, ———, and M. Castonguay. 1987. Reproductive sympatry of American and European eels and implications for migration and taxonomy. Am. Fish. Soc. Symp. **1:** 286–297.

Melià, P., M. Schiavina, M. Gatto, L. Bonaventura, S. Masina, and R. Casagrandi. 2013. Integrating field data into individual-based models of the migration of European eel larvae. Mar. Ecol. Prog. Ser. **487:** 135–149, doi:10.3354/meps10368

Miller, M. J. 2009. Ecology of anguilliform leptocephali: Remarkable transparent fish larvae of the ocean surface layer. Aqua-BioScience Monogr. **2:** 1–94.

Montgomery, J. C., A. Jeffs, S. D. Simpson, M. Meekan, and C. Tindle. 2006. Sound as an orientation cue for the pelagic larvae of reef fishes and decapod crustaceans. Adv. Mar. Biol. **51:** 143–196, doi:10.1016/S0065-2881(06)51003-X

Mouritsen, H., J. Atema, M. J. Kingsford, and G. Gerlach. 2013. Sun compass orientation helps coral reef fish larvae return to their natal reef. PLoS One **8:** e66039, doi:10.1371/journal.pone.0066039

Pacariz, S., H. Westerberg, and G. Björk. 2014. Climate change and passive transport of European eel larvae. Ecol. Freshw. Fish **23:** 86–94, doi:10.1111/eff.12048

Quinn, T. P. 1980. Evidence for celestial and magnetic compass orientation in lake migrating sockeye salmon fry. J. Comp. Physiol. **137:** 243–248, doi:10.1007/BF00657119

Righton, D., K. Aarestrup, D. Jellyman, P. Sébert, G. Van Den Thillart, and K. Tsukamoto. 2012. The *Anguilla* spp. migration problem: 40 million years of evolution and two millennia of speculation. J. Fish Biol. **81:** 365–386, doi:10.1111/j.1095-8649.2012.03373.x

Rypina, I. I., L. J. Pratt, and M. S. Lozier. 2011. Near-surface transport pathways in the North Atlantic Ocean: Looking for throughput from the subtropical to the subpolar gyre. J. Phys. Oceanogr. **41:** 911–925, doi:10.1175/2010JPO4498.1

Schmidt, J. 1923. The breeding places of the eel. Philos. Trans. R. Soc., B **211:** 179–208, doi:10.1098/rstb.1923.0004

———. 1931. Eels and conger eels of the North Atlantic. Nature **128:** 602–604, doi:10.1038/128602a0

Siegel, D., S. Mitarai, C. J. Costello, S. D. Gaines, B. E. Kendall, R. R. Warner, and K. B. Winters. 2008. The stochastic nature of larval connectivity among nearshore marine populations. Proc. Natl. Acad. Sci. USA **105:** 8974–8979, doi:10.1073/pnas.0802544105

Stobutzki, I., and D. Bellwood. 1998. Nocturnal orientation to reefs by late pelagic stage coral reef fishes. Coral Reefs **17:** 103–110, doi:10.1007/s003380050103

Sullivan, M., K. Able, J. Hare, and H. Walsh. 2006. *Anguilla rostrata* glass eel ingress into two, US east coast estuaries: Patterns, processes and implications for adult abundance. J. Fish Biol. **69:** 1081–1101, doi:10.1111/j.1095-8649.2006.01182.x

Tanaka, Y., K. Satoh, H. Yamada, T. Takebe, H. Nikaido, and S. Shiozawa. 2008. Assessment of the nutritional status of field-caught larval Pacific bluefin tuna by RNA/DNA ratio based on a starvation experiment of hatchery-reared fish. J. Exp. Mar. Biol. Ecol. **354:** 56–64, doi:10.1016/j.jembe.2007.10.007

Tesch, F. W. 2008. The eel, 5th ed. Blackwell.

———, T. Wendt, and L. Karlsson. 1992. Influence of geomagnetism on the activity and orientation of the eel, *Anguilla anguilla* (L.), as evident from laboratory experiments. Ecol. Freshw. Fish **1:** 52–60, doi:10.1111/j.1600-0633.1992.tb00007.x

Wang, C., and W. Tzeng. 2000. The timing of metamorphosis and growth rates of American and European eel leptocephali: A mechanism of larval segregative migration. Fish. Res. **46:** 191–205, doi:10.1016/S0165-7836(00)00146-6

Werner, F. E., R. I. Perry, R. G. Lough, and C. E. Naimie. 1996. Trophodynamic and advective influences on Georges Bank larval cod and haddock. Deep-Sea Res. II **43:** 1793–1822, doi:10.1016/S0967-0645(96)00042-2

Wiltschko, R., and W. Wiltschko. 1995. Magnetic orientation in animals. Springer Berlin.

Wuenschel, M., and K. Able. 2008. Swimming ability of eels (*Anguilla rostrata, Conger oceanicus*) at estuarine ingress: Contrasting patterns of cross-shelf transport? Mar. Biol. **154:** 775–786, doi:10.1007/s00227-008-0970-7

Yuan, G., L. Pratt, and C. Jones. 2004. Cross-jet Lagrangian transport and mixing in a 21/2-layer model. J. Phys. Oceanogr. **34:** 1991–2005, doi:10.1175/1520-0485(2004)034<1991:CLTAMI>2.0.CO;2

Associate editor: Craig. L. Stevens

Received: 07 March 2014
Accepted: 02 June 2014
Amended: 16 June 2014